Using super-resolution images to improve the measurement accuracy of DIC

Yueqi Wang[a], Pascal Lava[a], Dimitri Debruyne[a]

Abstract

DIC measurements highly depend on the intensity interpolation of images to achieve subpixel accuracies. The intensity interpolation at subpixel positions is based on the grey levels sampled at integer pixels. Therefore, the sampling rate is crucial to the interpolated intensities. The sampling rate is restricted by the camera resolution. With insufficient resolution, the interpolated intensities at subpixel positions evidently differ from the reality, and significantly degrade the measurement quality. In order to deal with this problem, we propose to use super-resolution images to improve the measurement accuracy when the camera resolution is insufficient. The concept of super-resolution is using a bunch of low-resolution images of a specimen to construct a high-resolution image. In this way, the interpolation error due to insufficient sampling rate can be compensated.

The conversion from the low-resolution images to the high-resolution one will introduce certain error. But it can be tested that the introduced error is far less significant than the improvement. Specifically, the technique is of important value for applications with high/ultra-high speed cameras, whereof the resolution is usually much lower compared to low speed cameras.

Contact information

[a] yueqi.wang@mtm.kuleuven.be
pascal.lava@mtm.kuleuven.be
dimitri.debruyne@mtm.kuleuven.be
KU Leuven Catholic University College Ghent
Gebroeders De Smetstraat 1, Ghent

Introduction

Measurement accuracy of the Digital Image Correlation (DIC) technique is of great importance for its applications. There are a number of investigations intended to study the measurement accuracy in the past, e.g. [1-7]. The subpixel accuracy of this technique is extensively discussed in these researches.

The principle of DIC is to retrieve the relationship between a deformed and a reference digital image according to the similarity of the intensities. Digital images, however, are not continuous but discrete samples of a specimen. In order to perform the correlation with subpixel accuracy, intensity interpolations are required to reconstruct the continuous sample of the specimen, so that intensities at subpixel positions can be estimated. The reconstruction, however, can never be exact, so that the obtained continuous sample is biased. In the signal processing field, this phenomenon is called *aliasing*. A bias in the displacement measurement is therefore introduced due to the biased reconstructed continuous sample. In this contribution, this error is named as the *aliasing error*. The rule of the thumb proposed by Sutton et al. [8] is also partly based on the consideration to reduce the *aliasing error*, which states:

"For accurate matching, image plane speckles should be sampled by at least a 3 by 3 pixel array to ensure minimal oversampling and reasonable intensity pattern reconstruction via interpolation."

The *aliasing error* can become remarkable if the speckle size is small.

In the field of signal processing, the *aliasing* effect can be compensated by *oversampling*, i.e. to keep the sampling rate much higher than the Nyquist frequency ($f_s >> f_N = 2B$, B is the bandlimit of a signal). In DIC, analogically, one can use high resolution cameras to achieve the *oversampling* and efficiently decrease the *aliasing error*. Modern cameras can have very high resolutions, which makes the problem not difficult to be solved for common applications despite the elevated costs. However, in the case of high/ultra high speed imaging, the resolution of high speed cameras has a trade-off between the pixel resolution and the camera speed. Taking the high speed camera Phantom V711 as an example, the resolution is reduced to 256×256 pixels at the speed of 187.2 KFPS. It is therefore worthy to find another solution to deal with the *aliasing error*.

In this contribution, we propose to use super-resolution (SR) images to improve the measurement accuracy, and the approach is denoted as SR DIC. A SR reference image is constructed from a number of low resolution (LR) images subjected to rigid motions. Image correlation is then performed between LR deformed images and the SR reference image to measure deformation. All the interpolations are done on the SR image, so that the *aliasing error* can be efficiently reduced. To validate the SR DIC approach, a virtual DIC test is also presented in this article.

Procedure of SR DIC

There are two kernel elements of SR DIC approach, i.e. creating a SR reference image and the correlation between images of different resolutions.

Creating a SR reference image

To perform a SR DIC, one captures a number of LR images at rigid motions w.r.t. a reference LR image. The rigid motions are either known, or measurable. All the LR images are then transferred to the same frame as the reference LR image according to the rigid motions, so that a virtual image with much denser pixels then a LR image is obtained. The virtual image has to be interpolated to a predefined regular mesh grid to construct a real SR reference image. The resolution of the SR image depends on the mesh grid. The procedure is schematically shown in Figure 1.

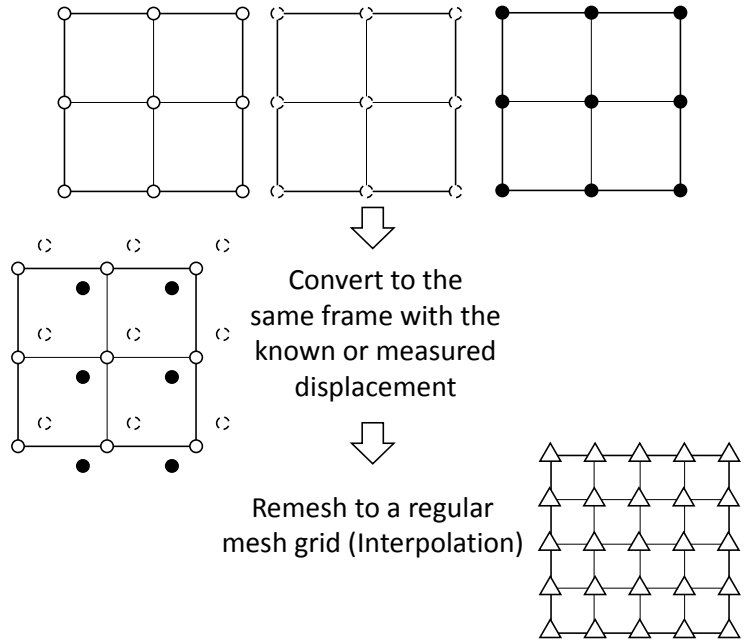

Figure 1: *Procedure of creating a SR image.*

Correlation between images of different resolutions

Once a SR reference image is obtained, one can measure the deformation of a deformed LR image by correlating to the SR image (Figure 2). The displacement is measured by minimizing the cost function:

$$C = \sum_{subset} \left(f\left((x, y), \mathbf{p}\right)_{SR} - g\left(x, y\right)_{LR} \right)^2 \tag{2.1}$$

where $f\left((x, y), \mathbf{p}\right)_{SR}$ is the intensity distribution of the SR reference image, $g\left(x, y\right)_{LR}$ is the intensity distribution of the LR deformed image, and $\mathbf{p}$ denotes the parameters of the

implemented shape function including the displacement (U,V) to be measured. The cost function is minimized by iterative methods, normally the Gauss-Newton method or the Levenberg–Marquardt method. $\mathbf{p}$ is then identified at the minimized cost function. It is noted that the measured displacement from $\mathbf{p}$ is actually the displacement of the SR image w.r.t. the LR image, which is the inverse of the real deformation. This should not be confused as the inverse compositional method that is described in [8,9]. In the current stage, we keep this inverse measurement. The conversion of this inverse field to a normal field will be investigated in future studies.

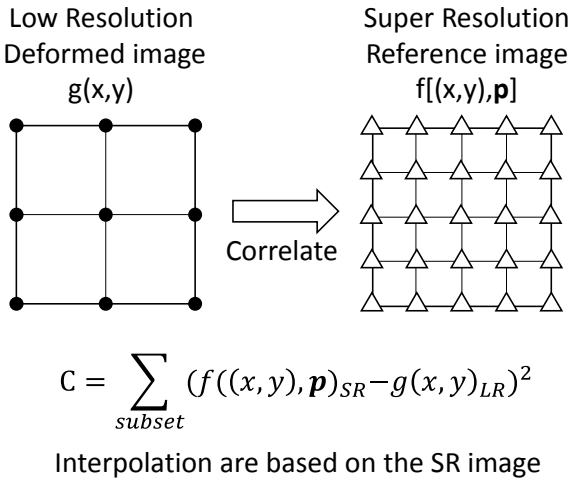

Figure 2: *Correlation between images of different resolutions.*

$f[(x,y),\mathbf{p}]_{SR}$ is probably located at subpixel positions, where intensity interpolation has to be performed. As the interpolation is based on the SR reference image, which possesses a higher sampling rate than the LR image, the *aliasing error* is expected to be reduced.

Temporal error and spatial error of subset-based DIC

It has been discussed in [10] that the measurement error in DIC should be distinguished as the temporal error and the spatial error, both of which include a bias and a random error. The subset-based DIC measures displacement for each subset individually, so that a bias and a random error are associated with this measurement of each subset. This error is denoted as the temporal measurement error. For the error of the horizontal displacement measured by a particular subset, it can be written as:

$$\Delta U_t = E(\Delta U_t) + \varepsilon(\Delta U_t) \tag{3.1}$$

where $E(\Delta U_t)$ is the temporal bias and $\varepsilon(\Delta U_t)$ is the temporal random error. $\varepsilon(\Delta U_t)$ is largely determined by the image noise, while $E(\Delta U_t)$ is determined by the intensity properties of this subset.

In the meanwhile, there is another measurement bias and random error, which evaluate the measurement of all the subsets in the zone of interest (ZOI):

$$\Delta U_s = E(\Delta U_s) + \varepsilon(\Delta U_s) \tag{3.2}$$

$E(\Delta U_s)$ is the spatial bias, which is the mean value of the temporal error ΔU_t of all the pixels, and $\varepsilon(\Delta U_s)$ is the spatial random error describes the variation of ΔU_t of all the pixels.

The random error is usually presented as the variance or the standard deviation of a random variable. Here we use $std(\Delta U_t)$ and $std(\Delta U_s)$ to describe the temporal and spatial random errors.

From [10] the temporal error is calculated as:

$$\Delta U_t = ([J_U]^T[J_U])^{-1}[J_U]^T[\Delta I^0] \tag{3.3}$$

where $[J_U]$ is a sub-matrix of the Jacobian matrix correspond to U, and $[\Delta I^0]$ is a column matrix contains the intensity errors of all the pixels in a subset.

The *aliasing* effect is included in the intensity error $[\Delta I^0]$. Therefore, the *aliasing error* is a part of the temporal error of the displacement measurement. The temporal error can thus be reduced by reducing the *aliasing error*, while the spatial error is also affected.

A virtual DIC test

A virtual DIC test is demonstrated in this section to validate the proposed method. Rigid motions of images are measured by both conventional DIC and SR DIC. The measurement results are then compared and discussed.

The creation of rigid motion images and the construction of a SR reference image

A speckle pattern is numerically created with the resolution of 4000×4000 pixels. The image is down-sampled to a 400×400 pixel image as the LR reference image by the image binning method [3]. With the same technique, 99 images are created at subpixel displacements in both horizontal and vertical directions ($U \in [0,0.9]$ pixels and $V \in [0,0.9]$ pixels) with the step size of 0.1 pixels (Figure 3). Gaussian random noise of $\sigma = 2$ grey levels are added to the images, which resembles common cameras for DIC tests. The speckle of the obtained LR images is evaluated by ImageJ [11], which shows that the speckle size is 9.5±3.7 pixels and the area coverage of the black patterns is 71.1%. Accordingly, the speckle pattern of the LR images fulfills the rule of the thumb.

The displacements of the 99 LR images are prescribed in this test, but they are probably not known in real applications. To motivate the use of the proposed SR DIC approach for general cases, these prescribed displacements are not applied to the construction of the SR image, but we measure the displacement by conventional DIC. The measurements are performed by the DIC package MatchID 2D [12], with the Gaussian image pre-filer and the cubic spline interpolation. The implemented parameters are listed in Table 1. The averaged displacement measurements

throughout the ZOI are considered as the displacement of the translated images. The spatial bias of the measurements is studied and shown in Figure 4, where one can observe that the measurement biases are less than 0.0015 pixels (Figure 4). It is worth to note that this error is not exceptionally low. E.g., even lower spatial biases have been reported in translation tests in [3,13] at similar conditions. With these DIC measurements, the 99 LR translated images are transformed to the frame of the LR reference image so that a virtual image is obtained. Gaussian interpolation is then performed to interpolate the virtual image to a regular mesh grid. Finally, a SR image with the resolution of 1600×1600 pixels is created.

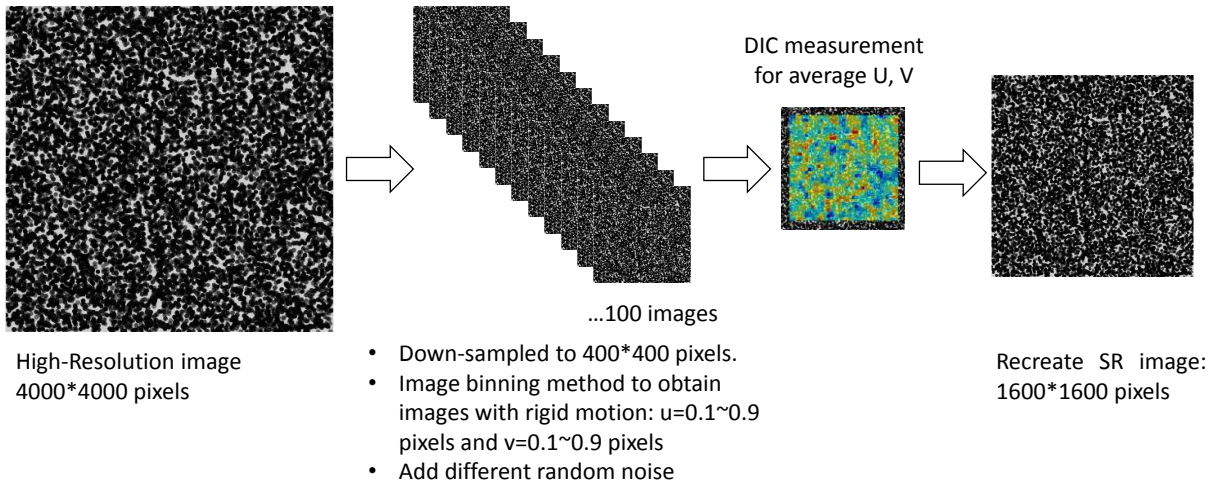

Figure 3: *Procedure of the construction of the SR reference images in the virtual test.*

	DIC implementation parameters	Specification
Image	Bit depth	8 bit
	Noise	2 Grey levels
Displacement	Matching criterion	Approximated NSSD
	Pre-filter	Gaussian σ_{pre}=1 pixel
	Interpolation	Cubic spline
	Shape function	Affine
	Subset size	21 Pixels
	Step size	10 pixels

Table 1: *DIC implementation parameters for measuring the displacement for the construction of the SR images*.

Displacement measurement

9 LR images with the vertical displacement of $V \in [0,0.9]$ are correlated with both the LR and the SR reference images. The correlation between the LR images are performed by MatchID 2D, with the same settings as shown in Table 1. For SR DIC, a code is programmed with less optimized parameters, i.e. with bi-cubic interpolation and without pre-filters, to correlate the images with different resolutions. The cost function is in the form of Equation (2.1), which is

minimized by the Gauss-Newton method. The convergence criterion is specified as the change of the parameters in $\mathbf{p}$ is less than 1%. All the other settings are the same as conventional DIC with LR images.

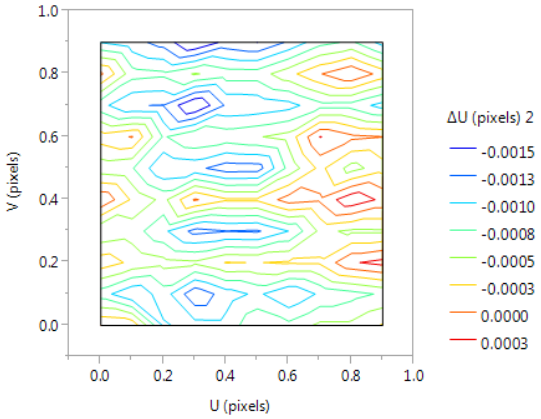

Figure 4: *Spatial bias of the horizontal displacement ΔU of the 99 rigid translated images with the noise level of 2 grey levels.*

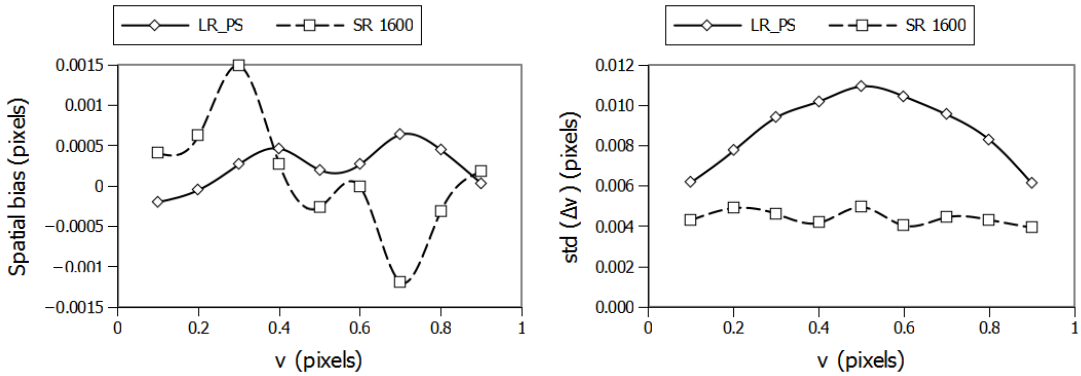

Figure 5: *Comparison between the spatial errors of the measurements from conventional DIC and SR DIC .*

Results and discussions

Figure 5 shows the comparison between the spatial errors of the measurements from conventional DIC and SR DIC. It can be observed that the spatial bias of the SR DIC is generally larger than that of conventional DIC. This is natural as the construction of the SR reference image is based on the conventional DIC measurements, so that the spatial bias of conventional DIC is already introduced in the SR reference image. As a consequence, the spatial bias of SR DIC cannot be improved.

Nevertheless, the spatial random error is significantly decreased by the SR DIC approach. The phenomenon can be explained as follows. The spatial random error is determined by the standard deviation of the temporal error. By SR DIC, the temporal error is reduced as the *aliasing error* is effectively compensated. Although the mean value of the temporal error, which is the spatial bias,

is not necessarily decreased, the standard deviation of it is significantly reduced. Finally the spatial random error is remarkably improved as a direct consequence.

The measurement error includes both the bias and the random error. It can be observed in Figure 5 that the spatial random error is much larger than the spatial bias. Therefore, it is the spatial random error which dominates the performance of DIC in this test. By using SR DIC, the spatial random error is significantly reduced while the spatial bias is slightly increased. In the end, the overall measurement error is remarkably decreased up to 50%.

Conclusion

In this article, a super-resolution (SR) DIC approach is presented in order to improve the measurement accuracy. By combining a number of low resolution images, a SR reference image is created, so that the sampling rate is increased. In this way, the *aliasing error* can be efficiently decreased, and the temporal error is therefore reduced. As such, the spatial random error, which can be presented as the standard deviation of the temporal error of all pixels, is also reduced. The SR DIC approach is validated by a virtual DIC test to measure the rigid translates. The measurement errors of conventional DIC and SR DIC are compared and discussed. It is found that compared to conventional DIC, the spatial bias of SR DIC measurements is not improved, whereas the spatial random error is significantly reduced. In all, SR DIC is capable to reduce the measurement error up to 50 % in this test.

References

[1] M. Bornert, F. Brémand, P. Doumalin, J-C Dupré, M. Fazzini, M. Grédiac, F. Hild, S. Mistou, J. Molimard, J-J Orteu, L. Robert, Y. Surrel, P. Vacher, and B. Wattrisse, Experimental mechanics **49**, 353-370 (2009).

[2] K. Triconnet, K. Derrien, F. Hild, and D. Baptiste, Optics and Lasers in Engineering **47**, 728-737, (2009).

[3] P.L. Reu, Experimental mechanics, **51**, 443-452, (2011).

[4] W. Tong, Strain, **41**, 167-175, (2005).

[5] B. Pan, H.M. Xie, Z.Y. Wang, K.M. Qian, and Z.Y. Wang, Optics express, **16**, 7037-7048, (2008).

[6] Y.Q. Wang, M.A. Sutton, H.A. Bruck, and H.W. Schreier, Strain, **45**, 160-178, (2009).

[7] G. Vendroux and W.G. Knauss, Experimental Mechanics, **38**, 86-92, (1998).

[8] M.A. Sutton, J.J. Orteu, and H.W. Schreier, *Image correlation for shape, motion and deformation measurements: basic concepts, theory and applications*, (Springer, 2009).

[9] B. Pan, L.P. Yu, D.F. Wu, and L.Q. Tang, Optics and Lasers in Engineering, **51**, 140-147, (2013).

[10] Y. Wang, P. Lava, P.L. Reu, P. Van Houtte, and D. Debruyne, Experimental Mechanics, under review.

[11] Image processing and analysis in java. http://rsbweb.nih.gov/ij/index.html

[12] MatchID, Metrology beyond color, http://www.matchidmbc.be/en

[13] B. Pan, Optics and Lasers in Engineering, **51**, 1161-1167, (2013).